Immunomodulatory glycan LNFPIII alleviates hepatosteatosis and insulin resistance through direct and indirect control of metabolic pathways

Published in final edited form as:
Nat Med. 2012 November ; 18(11): 1665–1672. doi:10.1038/nm.2962.

Immunomodulatory glycan LNFPIII alleviates hepatosteatosis and insulin resistance through direct and indirect control of metabolic pathways

Prerna Bhargava[1], **Changlin Li**[2], **Kristopher J. Stanya**[1], **David Jacobi**[1,3], **Lingling Dai**[1,4], **Sihao Liu**[1], **Matthew R. Gangl**[1], **Donald A. Harn**[2], and **Chih-Hao Lee**[1]

[1]Department of Genetics and Complex Diseases, Division of Biological Sciences, Harvard School of Public Health, 665 Huntington Ave, Boston, MA 02115, USA

[2]Department of Infectious Diseases, College of Veterinary Medicine, University of Georgia, Athens, GA 30602, USA

[3]CHRU de Tours, Service de Médecine Interne-Nutrition, INSERM U 1069, Université François Rabelais, Tours, France

[4]Pharmacogenetics Research Institute, Institute of Clinical Pharmacology, Central South University, Changsha, Hunan, People's Republic of China

Abstract

Parasitic worms express host-like glycans to attenuate the immune response of human hosts. The therapeutic potential of this immunomodulatory mechanism in controlling metabolic dysfunction associated with chronic inflammation remains unexplored. We demonstrate here that administration of Lacto-N-fucopentaose III (LNFPIII), a Lewis^X containing immunomodulatory glycan found in human milk and on parasitic helminths, improves glucose tolerance and insulin sensitivity in diet-induced obese mice. This effect is mediated partly through increased Il-10 production by LNFPIII activated macrophages and dendritic cells, which reduces white adipose tissue inflammation and sensitizes the insulin response of adipocytes. Concurrently, LNFPIII treatment up-regulates nuclear receptor Fxr-α (or Nr1h4) to suppress lipogenesis in the liver, conferring protection against hepatosteatosis. At the signaling level, the extracellular signal-regulated kinase (Erk)-Ap1 pathway appears to mediate the effects of LNFPIII on both inflammatory and metabolic pathways. Our results suggest that LNFPIII may provide novel therapeutic approaches to treat metabolic diseases.

Metabolic syndrome is a major medical and economic concern worldwide. Nutrient surplus is causative to the obesity pandemic as well as increased metabolic burdens in mitochondria and endoplasmic reticulum, leading to organelle dysfunction[1]. Chronic inflammation is a

Correspondence should be addressed: Chih-Hao Lee, PhD, Department of Genetics and Complex Diseases, Harvard School of Public Health, 665 Huntington Ave, Bldg1, Rm 207, Boston, MA 02115, USA. Phone: (617) 432-5778; Fax (617) 432-5236, clee@hsph.harvard.edu. Donald A. Harn, PhD, Department of Infectious Diseases, College of Veterinary Medicine, University of Georgia, Athens, GA 30602, USA. Phone: (706) 542-4569, dharn@uga.edu.

AUTHOR CONTRIBUTIONS

P.B was involved in experimental design and execution, data analyses and manuscript preparation. K.J.S., M.R.G. and C.L. conducted GTT and ITT with P.B. D.J. and L.D. provided technical assistance. S.L. assisted in hepatocyte isolations. C.L. provided LNFPIII and SEA preparations. D.A.H. helped with experimental design, data interpretation and manuscript writing. C.H.L directed the project, participated in data analyses and interpretation and wrote the manuscript.

COMPETING FINANCIAL INTERESTS

The authors declare no competing financial interests.

common outcome to these metabolic stresses and a key contributor of pathologies associated with metabolic diseases, such as insulin resistance, type 2 diabetes, atherosclerosis and nonalcoholic fatty liver diseases. Although features of chronic "metabolic-related inflammation" differ from those of acute inflammatory responses to exogenous insults, studies have shown that several pathogen sensing mechanisms of innate immunity are negative regulators of insulin sensitivity[1]. For example, pattern recognition receptors and downstream effectors [e.g., toll-like receptor-4 (Tlr4), IκB kinase β (Ikk-β) and Ikk-ε, Tnf-α and double-stranded RNA-dependent protein kinase] have been shown to be activated by high fat feeding and to induce metabolic diseases[2–6]. In addition, activation of the nucleotide-binding domain, leucine-rich-containing family, pyrin domain-containing-3 (Nlrp3) inflammasome, possibly in response to lipid metabolites (e.g., fatty acids and ceramides)[7,8], results in the cleavage of pro-caspase-1 (pro-Casp-1) and release of mature Il-1β, which causes insulin resistance[7,8].

Resident macrophages and lymphocytes in metabolic tissues, such as white adipose tissue (WAT) and liver, are believed to play important roles in metabolic-related inflammation[9–13]. Obesity triggers the infiltration of pro-inflammatory macrophages into WAT where they are histologically presented as crown-like structures[14,15]. These so called "classically activated" (or M1) macrophages are partly responsible for low-grade, chronic inflammation associated with metabolic dysregulation[1]. In contrast, adipose resident macrophages (ATMs) from lean individuals exhibit an "alternatively activated" (or M2) phenotype[16], which functions to repair damage inflicted by proinflammatory M1 signals[17]. Subsequent studies have identified several sources of Th2 cytokines (e.g., Il-4 and Il-13) within WAT that mediate alternative activation[10,13,18]. Depletion of Th2 cytokine producing cells or the downstream mediators in macrophages leads to insulin resistance[10,13,19]. In contrast, increased Th2 cytokine production as seen in helminth infection, improves glucose homeostasis[18]. While it remains unclear how Th2-biased, anti-inflammatory immune responses improve metabolic homeostasis, over-expression of the anti-inflammatory cytokine Il-10 has been shown to improve insulin sensitivity[20].

The ability to drive Th2-type and anti-inflammatory responses during helminth infection has been associated with decreased damage to host tissues, prolonging host survival[21]. During infection with *Schistosoma mansoni* (*S. mansoni*), parasite eggs trapped in host tissues, such as the liver, are the main stimuli for Th2 cytokine production in mice[22]. Injection of a saline soluble homogenate of eggs (or soluble egg antigen, SEA) is sufficient to induce Th2-biasing of the immune response[23]. Subsequently, it was shown that glycans and glycoproteins found in SEA, such as the Lewis^X containing Lacto-N-fucopentaose III (LNFPIII), LacdiNAc, fucosylated LacdiNac and omega-1 (a T2 RNase), are capable of mediating the immunomodulatory activity[24–27]. Notably, LNFPIII is one of the major sugars found in human milk post-partum and is thought to play a similar protective role in the fetus[28,29]. These observations suggest that during co-evolution with human hosts, *S. mansoni* parasites expressing immunomodulatory glycans were able to escape detection and had a developmental advantage. In fact, macrophages treated with LNFPIII exhibit a Th2 cytokine-independent, M2-like phenotype, characterized by the expression of the M2 markers, arginase 1 (Arg1) and Ym1[30]. LNFPIII and other helminth derived glycans induce Il-10 production[31], up-regulate T regulatory cell numbers[32] and inhibit bacterial lipopolysaccharide induced inflammatory responses[31]. The mechanisms through which LNFPIII exerts these anti-inflammatory activities remain poorly characterized. It has been shown that LNFPIII signals through several C-type lectin receptors[33] and Tlr4[34], which lead to activation of extracellular signal-regulated kinase (Erk). Although helminth infections polarize the immune response towards the Th2 type, studies have shown that it reduces, rather than exacerbates, the incidence of allergic responses, possibly because of the regulatory activity of Il-10[35].

In the current study, we seek to further characterize the unique immunomodulatory activity of LNFPIII and determine whether LNFPIII is effective in dampening chronic inflammation and improving metabolic function in a diet induced model of type 2 diabetes. Our results show LNFPIII or SEA treatment reduced inflammation and increased insulin sensitivity in WAT in an Il-10-dependent manner. Further, LNFPIII directly regulates the lipogenic program in hepatocytes and prevents obesity-induced hepatic steatosis through an unexpected link to the nuclear receptor Fxr-α.

RESULTS

LNFPIII treatment improves insulin sensitivity

LNFPIII has been shown to induce M2-like macrophage activation, independent of Th2 cytokines[30]. We confirmed that LNFPIII treatment up-regulated *Arg1*, *Ym1* and *Mgl1* expression, albeit to a lesser extent than Il-4, in macrophages (Fig. 1a). In contrast, LNFPIII was more effective than Il-4 in inducing *Il-10* expression and release into macrophage conditioned media (CM) (Fig. 1a,b and Supplementary Fig. 1a). This effect was blunted when we treated macrophages with PD98059 to block the activity of Erk, which has been implicated in mediating LNFPIII signal transduction (Fig. 1b)[31,34,36]. The Il-10 producing activity of LNFPIII was also observed in dendritic cells (Supplementary Fig. 1b) and was independent of Stat6 and Ppar-δ (known effectors of Th2 cytokines, Supplementary Fig. 1c). Taken together, LNFPIII induces an anti-inflammatory state that increases Il-10 production.

To determine whether the immunomodulatory activity of LNFPIII might be beneficial for treating metabolic diseases, we injected 8 week old male mice (C57BL/6) with vehicle or LNFPIII (25 μg, twice a week) for 4–6 weeks following onset of high fat diet (HFD) induced obesity and metabolic dysfunction. Consistent with the *in vitro* study, LNFPIII treated mice had higher circulating Il-10 concentrations, while Il-4 remained unchanged when compared to vehicle treated animals (Fig. 1c). When subjected to glucose tolerance test (GTT), LNFPIII treated mice showed significantly higher glucose handling capability versus the vehicle control group (Fig. 1d. Area under the curve, AUC: vehicle = 36,727.5 ± 1,769.13; LNFPIII = 29,244 ± 1,119.7, $P = 0.0159$). LNFPIII also improved insulin sensitivity, compared to vehicle treatment, as demonstrated by reductions in fasting serum insulin concentrations (vehicle: 1.54 ± 0.07; LNFPIII: 1.29 ± 0.06 ng ml^{-1}, $P < 0.05$) and improvement in insulin tolerance test (ITT, AUC: vehicle = 123.58 ± 4.79; LNFPIII = 98.23 ± 3.30, $P = 0.0357$) and the homeostasis model of assessment-insulin resistance (HOMA-IR) (Fig. 1e). Enhanced insulin signaling, based on insulin stimulated Ser473 Akt phosphorylation, was observed in WAT but not in liver or muscle (Fig. 1f,g and data not shown). We conducted parallel metabolic studies with SEA treatment, which led to higher circulating Il-10 and Il-4 concentrations (Supplementary Fig. 1d). High fat fed mice treated with SEA also displayed an improved insulin response determined by GTT, ITT, fasting insulin levels and HOMA-IR (Supplementary Fig. 1e–g). LNFPIII or SEA treatment did not affect body weight, food intake and circulating levels of lipids and adiponectin (Supplementary Table 1). These studies demonstrate the potential of using glycans derived from *S. mansoni* egg extract, including LNFPIII, to improve glucose homeostasis and insulin sensitivity.

LNFPIII enhances WAT insulin signaling through Il-10

The interaction between resident macrophages and adipocytes plays an important role in adipose tissue metabolic homeostasis[10]. WAT histological analyses demonstrated that mice given LNFPIII had lower numbers of crown-like structures and reduced expression of *F4/80* (a macrophage marker, Fig. 2a,b), compared to vehicle treated animals. In addition, *Il-10* and M2 genes (*Arg1* and *Mgl1*) were up-regulated, whereas *Tnf-α* and genes encoding the

inflammasome (*Casp-1*, *Nlrp3*, *Il-18*, and *Il-1β*) were down-regulated by LNFPIII treatment (Fig. 2b). Consistent with the increased insulin sensitivity, expression of insulin receptor β (*InsR-β*), insulin receptor substrate 2 (*Irs2*), *C/ebp-α*, glucose transporter 4 (*Glut4*) and lipogenic genes were higher in WAT from LNFPIII treated mice, compared to vehicle treated controls (Fig. 2c). C/ebp-α and Irs2 protein levels were also elevated (Fig. 2d). We obtained similar results in SEA treated cohorts (Supplementary Fig. 2). Of note, SEA induced *Arg1* expression in WAT to a greater extent than LNFPIII, reflecting the fact that SEA treatment increased serum Il-4 concentrations (Supplementary Fig. 1d). These data support the notion that LNFPIII modulates WAT resident macrophage inflammation and improves adipose tissue metabolic homeostasis.

Both *in vitro* and *in vivo* studies demonstrated that LNFPIII induced an anti-inflammatory phenotype characterized by elevated Il-10 concentrations, which has been shown to improve metabolic homeostasis[20]. To address whether the insulin sensitizing effect in WAT is a direct action of LNFPIII or mediated by Il-10, we cultured 3T3-L1 adipocytes ± LNFPIII or recombinant Il-10 (rIl-10). We observed that rIl-10, but not LNFPIII itself, improved insulin responsiveness determined by insulin stimulated Akt phosphorylation, glucose uptake and lipogenesis (Fig. 3a). CM from LNFPIII primed wild type (WT) macrophages, which contained higher Il-10 concentrations (Fig. 1b), was able to reproduce the insulin sensitizing activity in 3T3-L1 adipocytes, an effect abrogated in CM from LNFPIII primed *Il-10*$^{-/-}$ macrophages (Fig. 3b). Furthermore, CM derived from LNFPIII primed WT, but not *Il-10*$^{-/-}$, macrophages induced the expression of *InsR*, *Irs2* and *C/ebp-α* and suppressed *Il-1β* and *Tnf-α* in 3T3-L1 adipocytes (Fig. 3c). Reconstitution of rIl-10 in CM from *Il-10*$^{-/-}$ macrophages restored its ability to improve insulin stimulated glucose uptake and modulate metabolic and inflammatory gene expression (Fig. 3b,c). *In vivo*, LNFPIII was unable to improve insulin tolerance (Fig. 3d and Supplementary Table 1), enhance insulin stimulated glucose uptake (Fig. 3e) and inhibit WAT inflammation (Supplementary Fig. 3a,b) in *Il-10*$^{-/-}$ mice. In addition, *Il- 10*$^{-/-}$ mice were more insulin resistant compared to wt controls (Supplementary Fig. 3c). Reciprocally, rIl-10 injections (1μg, every other day for 3 doses) improved glucose tolerance and insulin sensitivity and recapitulated the WAT phenotype observed in LNFPIII treated mice (Supplementary Fig 3d–h and Supplementary Table 1). Taken together, the results suggest that Il-10 is required for LNFPIII mediated improvement in WAT insulin signaling and systemic glucose homeostasis.

LNFPIII protects against diet-induced hepatic steatosis

In addition to improving WAT function, histological and triglyceride content analyses showed a strong protective effect of LNFPIII against HFD-induced hepatic lipid accumulation, compared to vehicle treated mice (Fig. 4a). Furthermore, overall liver function, determined by circulating levels of alanine aminotransferase (ALT) and aspartate aminotransferase (AST), was substantially improved (Fig. 4b). In line with reduced hepatic steatosis, expression of lipogenic genes, including fatty acid synthase (*Fas*), acetyl-CoA carboxylase1/2 (*Acc1/2*), stearoyl-CoA desaturase 1 (*Scd1*) and sterol regulatory element-binding protein 1c (*Srebp-1c*), was lower in LNFPIII- versus vehicle-treated livers (Fig. 4c). Srebp-1c is a master lipogenic transcription factor whose expression and transcriptional activity are controlled by a network of nuclear receptor signaling pathways, notably, the positive regulator Lxr-α (Nr1h3)[37] and negative regulators Fxr-α (Nr1h4) and its target Shp (Nr0b2)[38]. *Fxr-α* consists of two major 5′ regulatory regions, with the upstream and downstream promoters driving the expression of *Fxr-α1/α2* and *Fxr-α3/α4* isoforms, respectively[39]. The only difference between Fxr-α1/α2 (or Fxr-α3/α4) is a 4 amino acid insertion in Fxr-α1 (or Fxr-α3). We found that expression of *Fxr-α3/α4* isoforms as well as several known Fxr target genes[39], including *Shp*, organic anion-transporting polypeptides (*Oatp*), phospholipid transfer protein (*Pltp*) and bile salt efflux pump (*Bsep*), were up-

regulated in livers of LNFPIII treated mice, compared to vehicle treated controls (Fig. 4c). *Lxr-α* expression remained unchanged. We obtained similar effects with SEA treatment, except that SEA up-regulated both *Fxr-α1/α2* and *Fxr-α3/α4* (Supplementary Fig. 4a–d). LNFPIII or SEA treatment did not alter metabolic gene expression in muscle (Supplementary Fig. 4e and data not shown). These results indicate that LNFPIII prevents ectopic fat accumulation in the liver and regulates the expression of transcriptional factors critical for *de novo* lipogenesis.

To assess the role of LNFPIII or LNFPIII primed macrophages in hepatic lipid homeostasis, we conducted lipogenic assays in isolated primary hepatocytes. LNFPIII, but not CM from LNFPIII treated macrophages, suppressed lipogenesis and increased fatty acid β-oxidation compared to the vehicle treatment (Fig. 5a). LNFPIII also induced *Fxr-α3/α4* and *Shp* as well as suppressed *Srebp-1c* and *Acc1* expression (Fig. 5b). Since LNFPIII did not affect β-oxidation gene expression (Fig. 4c and 5b), the increased fat burning was likely secondary to decreased fatty acid synthesis. These results suggest that unlike in WAT, the LNFPIII effect in the liver was not mediated by Il-10. Consistent with this notion, rIl-10 treatment did not affect hepatic de novo lipogenesis *in vitro* or *in vivo* (Supplementary Fig. 5a–c) and the protective effect of LNFPIII was preserved in *Il-10*$^{-/-}$ liver (Supplementary Fig 5d,e).

LNFPIII suppresses hepatic de novo lipogenesis through Fxr

The up-regulation of the Fxr-α-dependent transcription program by LNFPIII suggested that LNFPIII may induce Fxr-α to inhibit fat synthesis. In fact, in hepatocytes with *Fxr-α* gene ablation or Erk inhibition by PD98059, LNFPIII was unable to inhibit *de novo* lipogenesis and increase fat oxidation (Fig. 5c). Furthermore, the ability of LNFPIII to reduce hepatic triglyceride accumulation, improve liver function and suppress lipogenic gene expression was lost in *Fxr-α*$^{-/-}$ mice (Fig. 5d,e and Supplementary Fig. 5f), while the insulin sensitizing activity of LNFPIII was unaffected (Supplementary Fig. 5g–i and Supplementary Table 1). Together, the results suggest LNFPIII inhibits hepatic lipogenesis in a Fxr-α-dependent manner.

We next sought to determine if Fxr-α is a molecular target of LNFPIII. As mentioned earlier, both human and mouse *Fxr-α* contain two major promoters (Fig. 6a). The 5′ proximal regulatory sequences were highly conserved between mouse, rat and human *FXR-α* genes (Supplementary Fig. 6a). We examined the activities of reporters driven by upstream (promoter 1) or downstream (promoter 2) regulatory regions in HepG2 cells (human hepatoma cells). In accordance with the regulation of *Fxr-α* in the liver or isolated hepatocytes, LNFPIII activated human *FXR-α* promoter 2, while SEA induced the activity of both promoters (Fig. 6a). *In vivo*, Fxr-α protein levels were higher in liver lysates from LNFPIII versus vehicle treated mice (Fig 6a). Through serial deletion of promoter 2, we defined a minimal LNFPIII responsive region (approximately 130 bp upstream of the transcriptional start site) that contained consensus binding sites for C/EBP and AP1 (Supplementary Fig. 6a). Site directed mutagenesis experiments further identified two overlapping AP1 sites (located between −57 and −47 bp) that were required for the induction of *FXR-α* promoter 2 by LNFPIII (Fig. 6b and Supplemental Fig. 6b). Similarly, inhibition of Erk activation, which is upstream of AP-1, by PD98059 abolished the LNFPIII induced activity of *FXR-α* promoter 2. In concert, LNFPIII treatment increased levels of phospho-Erk and total Erk in the liver (Fig. 6c) and hepatocytes (Fig. 6d). Similar results were observed in SEA treated liver cells (Supplementary Fig. 6c–d). Collectively, these findings suggest that LNFPIII regulates hepatic lipogenesis through the Erk-Ap1-Fxr-α axis.

DISCUSSION

In this study, we demonstrate that LNPFIII (and SEA) alleviates the pathologies associated with HFD-induced obesity. LNFPIII treatment shifts the immune profile to an anti-inflammatory state and decreases macrophage infiltration in metabolic tissues of mice that have already become obese. This effect is, in part, driven by Il-10, which inhibits inflammation and enhances the insulin response in WAT. In the liver, LNFPIII up-regulates bile acid sensing nuclear receptor *Fxr-α* and its downstream targets. Activated Fxr-α signaling suppresses lipogenesis and protects against hepatic steatosis. Taken together, our results demonstrate a therapeutic potential for LNFPIII in treating components of metabolic syndrome through its ability to directly modulate both immune and metabolic pathways.

The hygiene hypothesis attributes the increased incidence of autoimmune diseases and allergic responses in developed countries to reduced human contact with pathogens[40]. A special emphasis has been on the interaction between parasitic worms and humans[40,41]; in addition to the Th2 biasing immune phenotype, helminth infections induce the proliferation of regulatory T cells and production of the anti-inflammatory cytokine Il-10[42]. Our data show that LNFPIII treatment is sufficient to increase Il-10 production in macrophages and dendritic cells. Regulatory T cells are likely another major source of Il-10[42]. These cells are enriched in fat tissues from lean individuals and play a role in maintaining WAT function[9]. Anti-inflammatory pathways are thought to improve metabolic homeostasis primarily through attenuating the action of pro-inflammatory signaling. Over-expression of Il-10 in the muscle was shown to improve systemic insulin resistance through suppression of inflammation[20]. We find that in an Il-10 dependent manner, CM from LNFPIII treated WT macrophages directly enhance insulin responses in adipocytes by up-regulation of *InsR* and *Irs2* and increase insulin mediated glucose uptake and lipogenesis. Acute rIl-10 injection in high fat fed mice also improves glucose homeostasis but does not affect WAT macrophage infiltration (data not shown), suggesting that the insulin sensitizing effect of Il-10 can be separated from its anti-inflammatory activity. Several studies have identified *IL-10* polymorphisms associated with insulin resistance/type 2 diabetes in humans[43,44]. Of note, a previous study has demonstrated that deficiency in hematopoietic cell derived Il-10 in mice through transplantation of *Il-10*$^{-/-}$ bone marrow does not affect high fat diet induced tissue inflammation and insulin resistance[45]. However, *Il-10* mRNA and protein levels are several-fold higher in WAT and liver in these mice, compared to animals receiving WT bone marrow. It is unclear whether the compensatory increase in Il-10 production is from non-hematopoietic cells or from residual WT bone marrow-derived cells. The result seems to suggest that increased Il-10 concentrations within metabolic tissues are sufficient to maintain metabolic homeostasis.

While adipose tissue is known to produce adipokines, such as leptin, adiponectin and resistin, to modulate systemic glucose and lipid metabolism, it is not a major tissue for glucose uptake under physiological conditions. LNFPIII treatment does not affect the expression of these adipokines in WAT (Supplementary Table 1 and data not shown). How does increased WAT insulin sensitivity by LNFPIII lead to improvement in systemic glucose homeostasis? It has been shown that GTT and ITT in muscle-specific insulin receptor knockout (MIRKO) mice are indistinguishable from control animals, even though insulin stimulated glucose uptake is substantially lower in muscle (the major site of glucose disposal)[46]. Subsequent studies attribute the normo-glycemic phenotype of MIRKO mice to a three-fold higher glucose deposition to WAT compared to control mice[47], suggesting that, at least in mice, increased glucose uptake by adipocytes is able to sustain glucose homeostasis. Consistent with this notion, over-expression of the glucose transporter Glut4 in adipose tissues improves glucose tolerance[48]. Recently, increased glucose flux in adipocytes has been shown to up-regulate fatty acid synthesis through a novel isoform of carbohydrate-

responsive-element-binding protein, Chrebp-β[49]. In addition, the expression of adipose *ChREBP-β* and lipogenic genes positively correlates with insulin sensitivity in humans[49]. Our data demonstrate that LNFPIII treatment increases WAT glucose uptake and lipogenic gene expression. *Chrebp-β* is also induced (data not shown). While the mechanism through which fat synthesis in adipose tissues contributes to whole body homeostasis is not completely understood, a lipogenic product of adipocytes has been linked to improved systemic metabolism[50]. The beneficial effect of LNFPIII could also be mediated by central regulation, in which reduced inflammation may lead to improved central insulin sensitivity that is known to regulate hepatic glucose production[51]. However, LNFPIII does not seem to affect gluconeogenesis based on pyruvate tolerance tests and the expression of gluconeogenic genes in the liver (data not shown).

After entering the body, *S. mansoni* settles in the hepatic portal system where male and female worms mate and produce eggs[22]. Egg deposition in the liver is critical for induction of a systemic Th2 response[22]. It is therefore not surprising that the liver is also a target of LNFPIII. At first glance, it seems unexpected that LNFPIII directly controls Fxr-α signaling to regulate hepatic lipid metabolism. Fxr-α senses endogenous bile acids and controls bile acid homeostasis by inhibiting production while increasing the recycling of bile acids in the enterohepatic system[52]. Fxr-α activation also suppresses lipogenesis through Shp-mediated inhibition of Srebp-1c in the liver[38]. Interestingly, *S. mansoni* is incapable of *de novo* synthesis of fatty acids and sterols but is able to synthesize complex lipids from precursors acquired from the host[53]. In addition, it has been shown that bile acids increase the number of deposited parasite eggs[54]. Therefore, the induction of Fxr-α by LNFPIII could be the host's response to limit fatty acids and bile acids available to the worm. In contrast, bile acids facilitate lipid absorption in the intestine. Increased bile flow via Fxr-α may help schistosomes to extract lipids from the digestive system of the host. Additionally, the induction of Fxr-α could serve as an anti-inflammatory mechanism in the liver as Fxr-α is known to trans-repress Nf-κb activity[55].

The signal transduction pathway of LNFPIII has not been fully characterized. In dendritic cells, LNFPIII is recognized by multiple C-type lectin receptors, including DC-SIGN, Mgl1 and mannose receptor. In addition, Erk is proposed to be a downstream effector of LNFPIII[31,56]. Erk-Ap1 has been shown to regulate Il-10 expression[36]. Indeed, the ability of LNFPIII to induce Il-10 production in the macrophage was blocked by Erk inhibition. We find that primary hepatocytes also express CLRs, such as DC-SIGN (data not shown) and LNFPIII is able to activate Erk in the liver, which mediates *Fxr-α* transcriptional regulation and the subsequent suppression of lipogenesis. The gene products of the two promoters (Fxr-α1/α2 versus Fxr-α3/α4) differ by several amino acids located at the N-terminus. Functional differences between isoforms have not been reported[39]. Our data suggests that the induction of Fxr-α3/α4 by LNFPIII is sufficient to suppress lipogenesis. While LNFPIII only activates the downstream *Fxr-α* promoter, SEA induces the activities of both promoters. This is not unexpected, since SEA is known to contain multiple bioactive glycans that could signal through different pathways[56]. Together, our data show that helminths may utilize the Erk-Ap1 signaling pathway to modulate host metabolism and immune responses (Fig. 6e). Our study suggests that the M2-like, anti-inflammatory activity of LNFPIII, which is likely the product of helminth's survival strategy, may be used to treat metabolic disorders, such as insulin resistance and nonalcoholic fatty liver diseases.

ONLINE METHODS

Animal experiments

We placed male C57BL/6J mice at 8–10 weeks of age (obtained from The Jackson Laboratory) on a high-fat, high-carbohydrate diet (F3282, Bio-Serv) for the duration of the

experiments. Six weeks after high fat feeding, we injected mice (i.p.) twice per week with 25 μg of dextran (40 kDa, vehicle) or LNFPIII conjugated to dextran (~8–10 LNFPIII per dextran). Experiments were reproduced in three independent mouse cohorts (n = 5–7 per treatment). We conducted similar metabolic experiments in three additional cohorts (n = 4–6 per treatment), which were given 0.9% NaCl (vehicle) or SEA dissolved in 0.9% NaCl (25 μg, twice a week). LNFPIII and SEA were prepared as described[30,57]. Metabolic studies started 4 weeks after LNFPIII or SEA treatment and were conducted after 6 h fasting. We sacrificed animals at the 6th week of treatment for serum and tissue collection. For rIl-10 experiments, mice were treated with PBS (vehicle) or rIl-10 (Peprotech; 1μg, i.p. every other day for a total of 3 doses) after 4 weeks of high fat diet. Body weight and food intake were monitored weekly. We performed GTT by injecting 1 g glucose per kg body weight into mouse peritoneum and measured blood glucose before and after injection at the time points indicated using a OneTouch glucose monitoring system (LifeScan). ITT was conducted similarly by injecting 1 U per kg body weight of insulin. *In vivo* insulin signaling was determined by injecting 5 U per kg body weight of insulin through the portal vein. We collected pieces of liver, epididymal fat and muscle before and 10 minutes after insulin injection and rapidly stored tissues in liquid nitrogen. Additional adipose tissue slices were immediately incubated with 2-[H^3]deoxy-D-glucose to determine insulin stimulated glucose uptake *ex vivo*. To estimate crown like structures, we divided one piece of epididymal fat pad into three sections and embedded them in a single paraffin block. We collected sequential sagittal sections every 20 μm for H&E staining. HOMA-IR was calculated as described[58]. Serum and tissue lipids, ALT and AST were measured using commercial kits as described previously[59]. We determined concentrations of p-Akt, t-Akt, insulin, Il-10 and Il-4 using ELISA-based plates from Meso Scale Discovery and Peprotech. The Dana-Farber/ Harvard Cancer Center Research Pathology Core provided all histological services and preliminary assessments by a pathologist. We obtained *Il-10*$^{-/-}$ and *Fxr-α*$^{-/-}$ mice (male, n = 6 per genotype per treatment, C57BL/6J background) from the Jackson Laboratory. Metabolic studies and treatments in these animals were similar to those in wt C57BL/6 mice. The Harvard Medical Area Standing Committee on Animals approved all the animal protocols.

Immunoblotting experiments

We performed Western blot analyses using antibodies to detect the following proteins: p-Akt (Cell Signaling # 9271, 1:1000); t-Akt (Cell signaling # 9272, 1:1000); Fxr-α (R&D systems, # PP-A9033A-00, Clone A9033A, 1:500 and Santa Cruz Biotechnology # sc-1204, 1:500); Irs-2 (Santa Cruz # sc-8299, 1:500); C/ebp-α (Santa Cruz # sc-61, 1:500); actin (Cell Signaling # 4970, Clone 13E5, 1:1000); tubulin (Cell Signaling # 2128, Clone 9F3, 1:1000). p-Erk (Cell signaling # 9101, 1:1000); t-Erk (Cell signaling # 4695, 1:1000).

Primary cells, adipocyte differentiation and functional assays

We differentiated bone marrow-derived macrophages in L929 conditioned media as previously described[10]. Dendritic cells were differentiated in the presence of M-CSF (3 ng mL^{-1}) and Il-4 (5 ng mL^{-1}). For CM, we treated cells with dextran (control) or LNFPIII (20 μg ml^{-1}) overnight. Following treatment, cells were washed and cultured in DMEM alone. We collected media 8 hours later and added 10% FBS, which constituted the CM. For M2 skewing experiments, we treated macrophages with dextran, LNFPIII (20 μg ml^{-1}) or Il-4 (20 ng ml^{-1}) overnight. Where indicated, cells were pretreated for 1 hour with PD98059 (10 μM, Cell Signaling) prior to treatments. PD98059 is an MEK1 (also called MAPKK or Erk kinase) inhibitor used to block Erk activation. We differentiated 3T3L1 cells in a cocktail containing insulin, isobutylmethylxanthine, and dexamethasone. For differentiation experiments, 3T3-L1 cells were given various treatments indicated together with the differentiation cocktail. At day 2, the cocktail was removed and differentiation continued in

the presence of the treatment and insulin. We performed TG analysis after 6 days of differentiation. Cellular lipids were extracted with a 2:1 (v/v) chloroform:methanol solution. For insulin signaling experiments, we treated fully differentiated 3T3-L1 adipocytes (at day 6) with the indicated treatments for 48 hr without insulin. Cells were washed, serum starved for 2 h and stimulated with insulin (100 nM) for 60 min. We conducted glucose uptake using 2-[H^3]deoxy-D-glucose with a 20 min insulin pre-stimulation. Cellular radioactivity was determined and normalized to protein content. Primary hepatocytes were isolated as previously described[59,60]. Hepatocytes were allowed to attach overnight in William's E, 5% FBS, followed by treatments for 24 h. For *de novo* lipogenesis, we labeled cells with ^{14}C-acetate and extracted lipids with a 2:1 (v/v) chloroform:methanol mixture 6 h later. β-oxidation was conducted as described previously[60]. For LNFPIII signaling, attached hepatocytes were pretreated with Erk inhibitor where indicated for 1 hr followed by a 30 min incubation with dextran or LNFPIII.

Expression analyses

For gene expression analyses, we determined relative expression levels using SYBR green-based real-time quantitative PCR (q-PCR) reactions. We used *36B4* levels for normalization. For western blot analyses, we prepared tissue and cell lysates in the presence of protease and phosphatase inhibitors. The four *Fxr-α* (*Nr1h4*) isoforms were based on previous reports, which were originally designated as *Fxr-α1/α2* and *Fxr-β1/β2*. The latter were renamed as *Fxr-α3/α4* to avoid confusion with the rodent *Fxr-β* (*Nr1h5*)[39]. For reporter assays, we cloned the upstream promoter 1 and downstream promoter 2 regions of human *FXR-α* gene into the pGL3-basic luciferase reporter vector and conducted transient transfection in HepG2 cells in a 96-well format. We used a β-galactosidase reporter construct for normalization.

Statistical analyses

Statistical analyses comparing two parameters (between treatments or genotypes) in cell-based work were conducted using the two-tailed Student's *t* test. Two parameters analyses for samples from *in vivo* studies (non-gaussian distribution) were determined using the Mann-Whitney test (Figs. 1c, 1g, 2a–d, 3e, 4a–c, 5d–e, 6c, Supplementary Figs. 1d, 1g, 2b–c, 3a, 3b, 3f–h, 4a–d, 5d–e, 5i and Supplementary Table 1). Statistics for multi-parameter analyses was determined by One-Way ANOVA followed by Bonferroni posthoc tests (Figs. 1a, 3a–c, 5a, 5c, 6a, 6d and Supplementary Figs. 1a, 5a, 6c–d). Two-way ANOVA was used to determine statistical significance for GTT and ITT (Figs. 1d–e, 3d and Supplementary Figs. 1e–f, 3c–e, 5f–g). Values are presented as mean ± SEM. For *in vitro* assays, the mean and SEM were determined from 3–4 biological replicates for one representative experiment. Experiments were repeated at least three times. $P < 0.05$ was considered significant.

Supplementary Material

Refer to Web version on PubMed Central for supplementary material.

Acknowledgments

We thank E. Hu, and S.M. Reilly for technical support and T. Horng (Harvard School of Public Health) for providing reagents. P. Bhargava and K. Stanya were supported by US National Institute of Health training grant (T32ES016645). This work was supported by: American Diabetes Association, American Heart Association and US National Institute of Health grant (R01DK075046) (C.-H.L.).

References

1. Gregor MF, Hotamisligil GS. Inflammatory mechanisms in obesity. Annu Rev Immunol. 29:415–445. [PubMed: 21219177]

2. Arkan MC, et al. IKK-beta links inflammation to obesity-induced insulin resistance. Nat Med. 2005; 11:191–198. [PubMed: 15685170]
3. Cai D, et al. Local and systemic insulin resistance resulting from hepatic activation of IKK-beta and NF-kappaB. Nat Med. 2005; 11:183–190. [PubMed: 15685173]
4. Chiang SH, et al. The protein kinase IKKepsilon regulates energy balance in obese mice. Cell. 2009; 138:961–975. [PubMed: 19737522]
5. Nakamura T, et al. Double-stranded RNA-dependent protein kinase links pathogen sensing with stress and metabolic homeostasis. Cell. 2010; 140:338–348. [PubMed: 20144759]
6. Shi H, et al. TLR4 links innate immunity and fatty acid-induced insulin resistance. J Clin Invest. 2006; 116:3015–3025. [PubMed: 17053832]
7. Vandanmagsar B, et al. The NLRP3 inflammasome instigates obesity-induced inflammation and insulin resistance. Nat Med. 2011; 17:179–188. [PubMed: 21217695]
8. Wen H, et al. Fatty acid-induced NLRP3-ASC inflammasome activation interferes with insulin signaling. Nat Immunol. 2011; 12:408–415. [PubMed: 21478880]
9. Feuerer M, et al. Lean, but not obese, fat is enriched for a unique population of regulatory T cells that affect metabolic parameters. Nat Med. 2009; 15:930–939. [PubMed: 19633656]
10. Kang K, et al. Adipocyte-derived Th2 cytokines and myeloid PPARdelta regulate macrophage polarization and insulin sensitivity. Cell Metab. 2008; 7:485–495. [PubMed: 18522830]
11. Nishimura S, et al. CD8+ effector T cells contribute to macrophage recruitment and adipose tissue inflammation in obesity. Nat Med. 2009; 15:914–920. [PubMed: 19633658]
12. Odegaard JI, et al. Alternative M2 activation of Kupffer cells by PPARdelta ameliorates obesity-induced insulin resistance. Cell Metab. 2008; 7:496–507. [PubMed: 18522831]
13. Winer S, et al. Normalization of obesity-associated insulin resistance through immunotherapy. Nat Med. 2009; 15:921–929. [PubMed: 19633657]
14. Weisberg SP, et al. Obesity is associated with macrophage accumulation in adipose tissue. J Clin Invest. 2003; 112:1796–1808. [PubMed: 14679176]
15. Xu H, et al. Chronic inflammation in fat plays a crucial role in the development of obesity-related insulin resistance. J Clin Invest. 2003; 112:1821–1830. [PubMed: 14679177]
16. Lumeng CN, Bodzin JL, Saltiel AR. Obesity induces a phenotypic switch in adipose tissue macrophage polarization. J Clin Invest. 2007; 117:175–184. [PubMed: 17200717]
17. Gordon S. Alternative activation of macrophages. Nat Rev Immunol. 2003; 3:23–35. [PubMed: 12511873]
18. Wu D, et al. Eosinophils sustain adipose alternatively activated macrophages associated with glucose homeostasis. Science. 2011; 332:243–247. [PubMed: 21436399]
19. Odegaard JI, et al. Macrophage-specific PPARgamma controls alternative activation and improves insulin resistance. Nature. 2007; 447:1116–1120. [PubMed: 17515919]
20. Hong EG, et al. Interleukin-10 prevents diet-induced insulin resistance by attenuating macrophage and cytokine response in skeletal muscle. Diabetes. 2009; 58:2525–2535. [PubMed: 19690064]
21. Herbert DR, et al. Alternative macrophage activation is essential for survival during schistosomiasis and downmodulates T helper 1 responses and immunopathology. Immunity. 2004; 20:623–635. [PubMed: 15142530]
22. Grzych JM, et al. Egg deposition is the major stimulus for the production of Th2 cytokines in murine schistosomiasis mansoni. J Immunol. 1991; 146:1322–1327. [PubMed: 1825109]
23. Okano M, Satoskar AR, Nishizaki K, Abe M, Harn DA Jr. Induction of Th2 responses and IgE is largely due to carbohydrates functioning as adjuvants on Schistosoma mansoni egg antigens. J Immunol. 1999; 163:6712–6717. [PubMed: 10586068]
24. Atochina O, Daly-Engel T, Piskorska D, McGuire E, Harn DA. A schistosome-expressed immunomodulatory glycoconjugate expands peritoneal Gr1(+) macrophages that suppress naive CD4(+) T cell proliferation via an IFN-gamma and nitric oxide-dependent mechanism. J Immunol. 2001; 167:4293–4302. [PubMed: 11591752]
25. Everts B, et al. Omega-1, a glycoprotein secreted by Schistosoma mansoni eggs, drives Th2 responses. J Exp Med. 2009; 206:1673–1680. [PubMed: 19635864]

26. Steinfelder S, et al. The major component in schistosome eggs responsible for conditioning dendritic cells for Th2 polarization is a T2 ribonuclease (omega-1). J Exp Med. 2009; 206:1681–1690. [PubMed: 19635859]
27. Van der Kleij D, et al. Triggering of innate immune responses by schistosome egg glycolipids and their carbohydrate epitope GalNAc beta 1-4(Fuc alpha 1-2Fuc alpha 1-3)GlcNAc. J Infect Dis. 2002; 185:531–539. [PubMed: 11865406]
28. Ko AI, Drager UC, Harn DA. A Schistosoma mansoni epitope recognized by a protective monoclonal antibody is identical to the stage-specific embryonic antigen 1. Proc Natl Acad Sci U S A. 1990; 87:4159–4163. [PubMed: 1971946]
29. Stahl B, et al. Oligosaccharides from human milk as revealed by matrix-assisted laser desorption/ionization mass spectrometry. Anal Biochem. 1994; 223:218–226. [PubMed: 7887467]
30. Atochina O, Da'dara AA, Walker M, Harn DA. The immunomodulatory glycan LNFPIII initiates alternative activation of murine macrophages in vivo. Immunology. 2008; 125:111–121. [PubMed: 18373667]
31. Harn DA, McDonald J, Atochina O, Da'dara AA. Modulation of host immune responses by helminth glycans. Immunol Rev. 2009; 230:247–257. [PubMed: 19594641]
32. Dutta P, et al. Lacto-N-fucopentaose III, a pentasaccharide, prolongs heart transplant survival. Transplantation. 2010; 90:1071–1078. [PubMed: 20885339]
33. van Liempt E, et al. Schistosoma mansoni soluble egg antigens are internalized by human dendritic cells through multiple C-type lectins and suppress TLR-induced dendritic cell activation. Mol Immunol. 2007; 44:2605–2615. [PubMed: 17241663]
34. Thomas PG, et al. Maturation of dendritic cell 2 phenotype by a helminth glycan uses a Toll-like receptor 4-dependent mechanism. J Immunol. 2003; 171:5837–5841. [PubMed: 14634093]
35. Schnoeller C, et al. A helminth immunomodulator reduces allergic and inflammatory responses by induction of IL-10-producing macrophages. J Immunol. 2008; 180:4265–4272. [PubMed: 18322239]
36. Dillon S, et al. A Toll-like receptor 2 ligand stimulates Th2 responses in vivo, via induction of extracellular signal-regulated kinase mitogen-activated protein kinase and c-Fos in dendritic cells. J Immunol. 2004; 172:4733–4743. [PubMed: 15067049]
37. Repa JJ, et al. Regulation of mouse sterol regulatory element-binding protein-1c gene (SREBP-1c) by oxysterol receptors, LXRalpha and LXRbeta. Genes Dev. 2000; 14:2819–2830. [PubMed: 11090130]
38. Watanabe M, et al. Bile acids lower triglyceride levels via a pathway involving FXR, SHP, and SREBP-1c. J Clin Invest. 2004; 113:1408–1418. [PubMed: 15146238]
39. Zhang Y, Kast-Woelbern HR, Edwards PA. Natural structural variants of the nuclear receptor farnesoid X receptor affect transcriptional activation. J Biol Chem. 2003; 278:104–110. [PubMed: 12393883]
40. Zaccone P, Fehervari Z, Phillips JM, Dunne DW, Cooke A. Parasitic worms and inflammatory diseases. Parasite Immunol. 2006; 28:515–523. [PubMed: 16965287]
41. Dunne DW, Cooke A. A worm's eye view of the immune system: consequences for evolution of human autoimmune disease. Nat Rev Immunol. 2005; 5:420–426. [PubMed: 15864275]
42. Hesse M, et al. The pathogenesis of schistosomiasis is controlled by cooperating IL-10-producing innate effector and regulatory T cells. J Immunol. 2004; 172:3157–3166. [PubMed: 14978122]
43. Bassols J, et al. Environmental and genetic factors influence the relationship between circulating IL-10 and obesity phenotypes. Obesity. 2010; 18:611–618. [PubMed: 19798061]
44. Chang YH, Huang CN, Wu CY, Shiau MY. Association of interleukin-10 A-592C and T-819C polymorphisms with type 2 diabetes mellitus. Hum Immunol. 2005; 66:1258–1263. [PubMed: 16690414]
45. Kowalski GM, et al. Deficiency of haematopoietic-cell-derived IL-10 does not exacerbate high-fat-diet-induced inflammation or insulin resistance in mice. Diabetologia. 2011; 54:888–899. [PubMed: 21210076]
46. Bruning JC, et al. A muscle-specific insulin receptor knockout exhibits features of the metabolic syndrome of NIDDM without altering glucose tolerance. Mol Cell. 1998; 2:559–569. [PubMed: 9844629]

47. Kim JK, et al. Redistribution of substrates to adipose tissue promotes obesity in mice with selective insulin resistance in muscle. J Clin Invest. 2000; 105:1791–1797. [PubMed: 10862794]
48. Shepherd PR, et al. Adipose cell hyperplasia and enhanced glucose disposal in transgenic mice overexpressing GLUT4 selectively in adipose tissue. J Biol Chem. 1993; 268:22243–22246. [PubMed: 8226728]
49. Herman MA, et al. A novel ChREBP isoform in adipose tissue regulates systemic glucose metabolism. Nature. 484:333–338. [PubMed: 22466288]
50. Cao H, et al. Identification of a lipokine, a lipid hormone linking adipose tissue to systemic metabolism. Cell. 2008; 134:933–944. [PubMed: 18805087]
51. Porte D Jr, Baskin DG, Schwartz MW. Insulin signaling in the central nervous system: a critical role in metabolic homeostasis and disease from C. elegans to humans. Diabetes. 2005; 54:1264–1276. [PubMed: 15855309]
52. Lefebvre P, Cariou B, Lien F, Kuipers F, Staels B. Role of bile acids and bile acid receptors in metabolic regulation. Physiol Rev. 2009; 89:147–191. [PubMed: 19126757]
53. Berriman M, et al. The genome of the blood fluke Schistosoma mansoni. Nature. 2009; 460:352–358. [PubMed: 19606141]
54. Badr SG, Pica-Mattoccia L, Moroni R, Angelico M, Cioli D. Effect of bile salts on oviposition in vitro by Schistosoma mansoni. Parasitol Res. 1999; 85:421–423. [PubMed: 10227062]
55. Wang YD, et al. Farnesoid X receptor antagonizes nuclear factor kappaB in hepatic inflammatory response. Hepatology. 2008; 48:1632–1643. [PubMed: 18972444]
56. Harnett W, Harnett MM. Helminth-derived immunomodulators: can understanding the worm produce the pill? Nat Rev Immunol. 2010; 10:278–284. [PubMed: 20224568]
57. Harn DA, Mitsuyama M, David JR. Schistosoma mansoni. Anti-egg monoclonal antibodies protect against cercarial challenge in vivo. J Exp Med. 1984; 159:1371–1387. [PubMed: 6538899]
58. Foss-Freitas MC, Foss MC. Comparison of the homeostasis model assessment and quantitative insulin sensitivity check index with data from forearm metabolic studies for the in vivo assessment of insulin sensitivity. Braz J Med Biol Res. 2004; 37:663–668. [PubMed: 15107927]
59. Liu S, et al. Role of peroxisome proliferator-activated receptor {delta}/{beta} in hepatic metabolic regulation. J Biol Chem. 2011; 286:1237–1247. [PubMed: 21059653]
60. Reilly SM, et al. Nuclear receptor corepressor SMRT regulates mitochondrial oxidative metabolism and mediates aging-related metabolic deterioration. Cell metab. 2010; 12:643–653. [PubMed: 21109196]

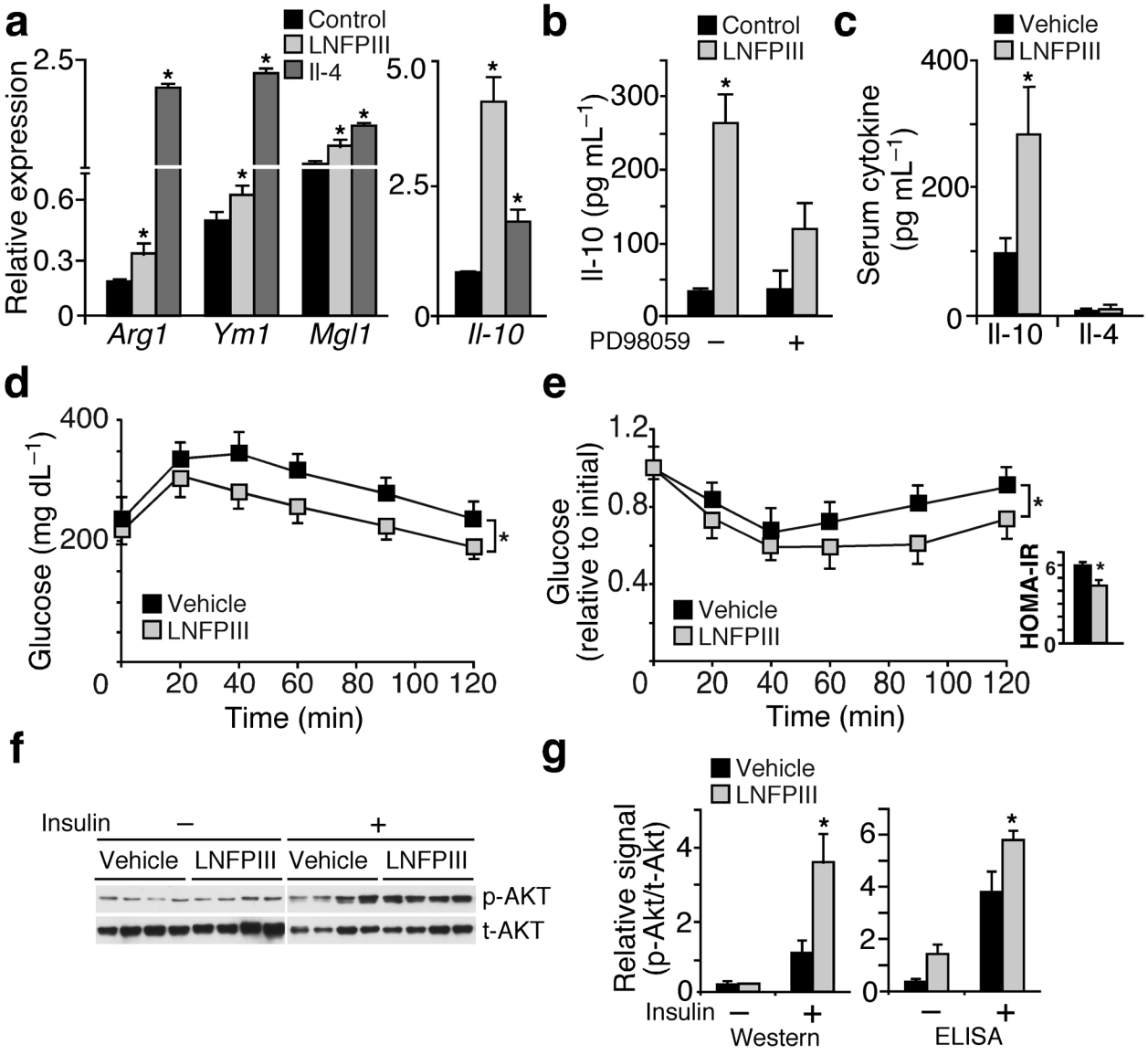

Figure 1.

LNFPIII increases Il-10 production and improves insulin sensitivity. (**a**) Real-time q-PCR examining the expression of M2 (alternative activation) genes in bone marrow derived macrophages treated with Il-4 (20 ng ml^{-1}) or LNFPIII (20 μg ml^{-1}) for 24 hr. (**b**) Il-10 concentrations in conditioned medium from LNFPIII or vehicle treated macrophages determined by ELISA. PD98059 (10 μM): Erk inhibitor. (**c**) Serum Il-10 and Il-4 concentrations in vehicle or LNFPIII treated mice (n = 5–7 per treatment) (**d** and **e**) Glucose tolerance test (GTT, **d**) and insulin tolerance test (ITT, **e**) in vehicle and LNFPIII treated mice. Inset in (**e**): homeostasis model of assessment-insulin resistance (HOMA-IR). (**f**) Western blot analyses to examine insulin stimulated Akt phosphorylation in WAT from vehicle and LNFPIII treated mice (from four individual mice per treatment). p-Akt: phospho-Akt; t-Akt: total Akt. (**g**) The relative level of p-Akt to t-Akt in WAT ±insulin injection quantified by densitometry based on Western signals in (f) or by ELISA-based assays. Values are expressed as means ± SEM. For *in vitro* assays, the mean and SEM were determined from 3–4 biological replicates for a representative experiment. Experiments

were repeated 3 times. *In vivo* studies were reproduced in three mouse cohorts (n = 5–7 per treatment). Insulin signaling was examined in two of the three cohorts. *P < 0.05 (LNFPIII or Il-4 versus vehicle control).

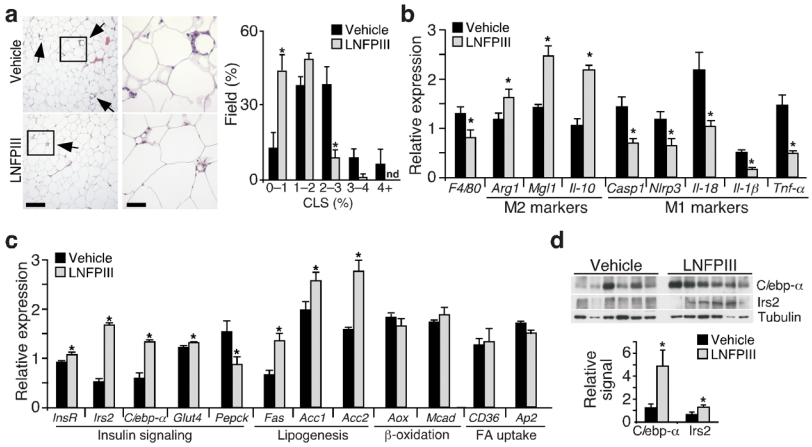

Figure 2.

Reduced inflammation and enhanced insulin signaling in WAT of LNFPIII treated mice. (**a**) Left panel: WAT histology showing crown-like structures (CLS, indicated with arrows). Scale bar: left images = 400 μm; right images = 100 μm. Right panel: CLSs quantified in 90 fields from 30 sections (3 fields per section) for each individual animal ($n = 4$ per group). Y-axis: % fields that contains certain percentage of CLSs; X-axis: % CLS-containing adipocytes in a given field; n.d: not detected. (**b**) Real-time q-PCR analyses of M1 and M2 gene expression in WAT of vehicle- and LNFPIII-treated mice ($n = 5$ per treatment). (**c**) Metabolic gene expression in WAT determined by real-time q-PCR. (**d**) Western blotting showing C/ebp-α and Irs2 protein levels in WAT. Bottom panel: relative C/ebp-α and Irs2 levels normalized to tubulin. Values are expressed as means ±SEM. Metabolic studies were reproduced in three mouse cohorts ($n = 5$–7 per treatment). Crown-like structures and expression analyses were examined in one and three of the three cohorts, respectively. *$P <$ 0.05 (LNFPIII versus vehicle).

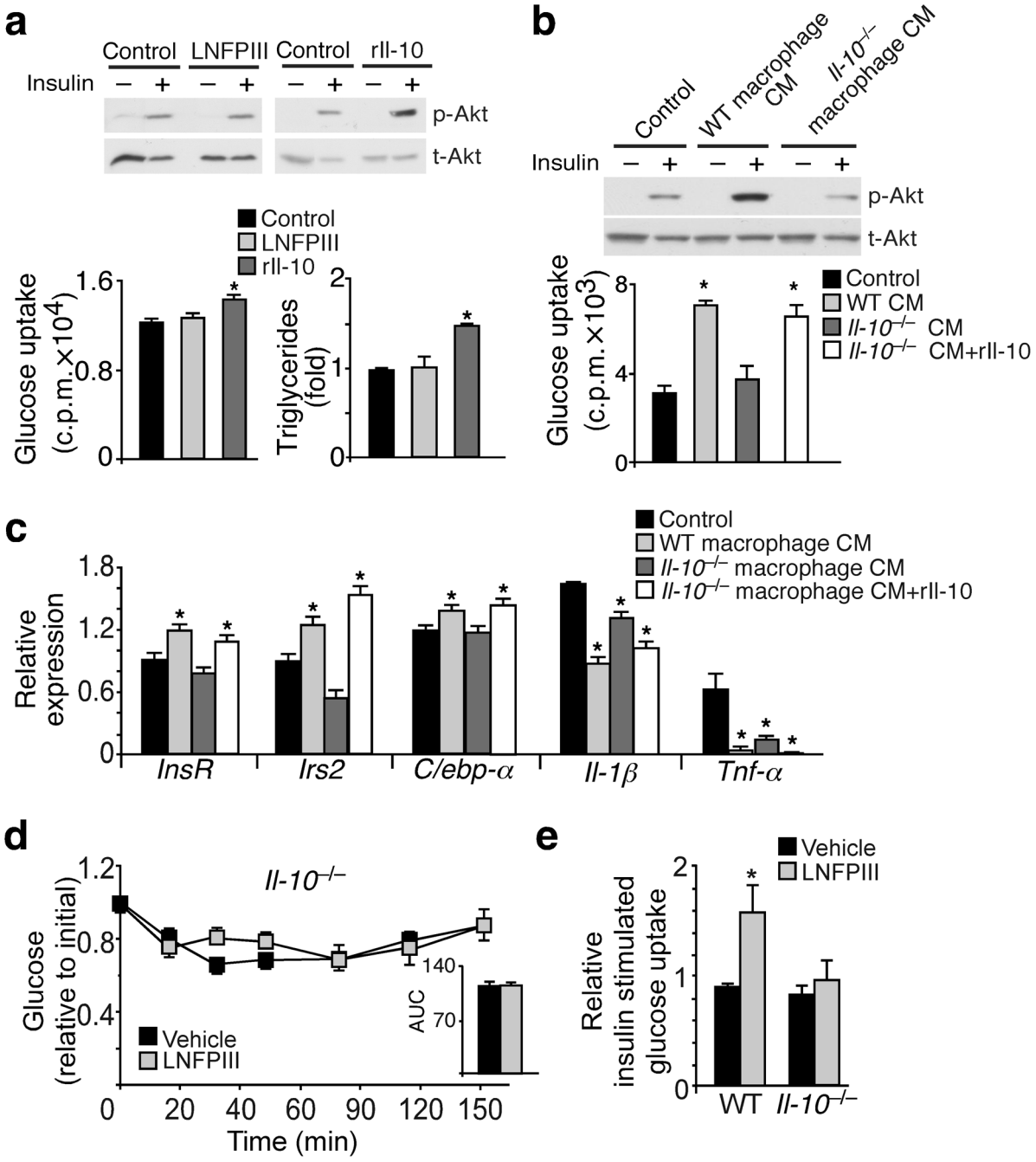

Figure 3.

LNFPIII primed macrophage conditioned medium improves insulin sensitivity in 3T3L1 adipocytes in an Il-10 dependent manner. (**a**) Top panel: Western blotting showing protein levels of total Akt (t-Akt) and insulin stimulated Akt phosphorylation (p-Akt) in 3T3-L1 adipocytes treated with vehicle, LNFPIII or rIl-10 (representative samples from three experiments each with three biological replicates). Bottom left panel: insulin stimulated glucose uptake determined using radioactive 2-[H^3]deoxy-D-glucose. Bottom right panel: cellular triglyceride contents measured at day 6 of 3T3-L1 adipocyte differentiation. Vehicle controls for LNFPIII (20 μg ml^{-1}) and Il-10 (10 ng ml^{-1}) were dextran and PBS,

respectively. (**b**) Top panel: Western blotting showing protein levels of t-Akt and insulin stimulated p-Akt in adipocytes treated with control and conditioned medium (CM) from LNFPIII primed wt and *Il-10*$^{-/-}$ macrophages. Bottom panel: insulin stimulated glucose uptake in adipocytes. (**c**) Gene expression in 3T3-L1 adipocytes determined by real-time q-PCR. (**d**) Insulin tolerance test in vehicle and LNFPIII treated *Il-10*$^{-/-}$ mice ($n = 6$ per treatment per genotype). AUC: area under the curve of ITT. (**e**) *Ex vivo* glucose uptake assay performed in adipose tissue slices collected before and after portal vein injection of 5 U kg^{-1} insulin. Values are expressed as means ±SEM. For *in vitro* assays, the mean and SEM were determined from 3–4 biological replicates for a representative experiment. Experiments were repeated three times. Studies in *Il-10*$^{-/-}$ and control mice were conducted in one cohort ($n = 6$). *$P < 0.05$ (treatment versus control).

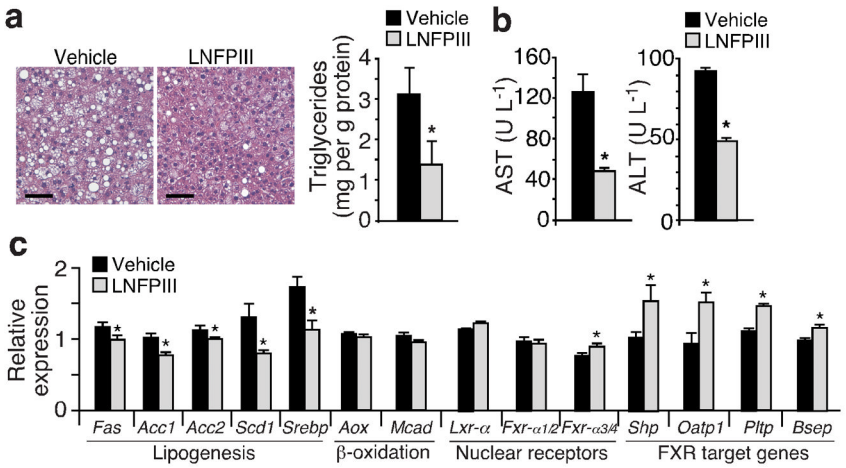

Figure 4.

LNFPIII protects against high fat diet induced hepatic steatosis. (**a**) Liver histology and triglyceride content analyses to determine hepatic fat accumulation in vehicle and LNFPIII treated mice. Scale bar = 100 μm. (**b**) Circulating AST and ALT concentrations to assess liver function. (**c**) Gene expression analyses in livers from vehicle or LNFPIII treated mice ($n = 5$) by real-time q-PCR. Values are expressed as means ±SEM. Metabolic studies were reproduced in three mouse cohorts ($n = 5$–7 per treatment). Histology was examined in one and lipid and expression analyses were examined in three of the three cohorts. $^*P < 0.05$ (LNFPIII versus vehicle control).

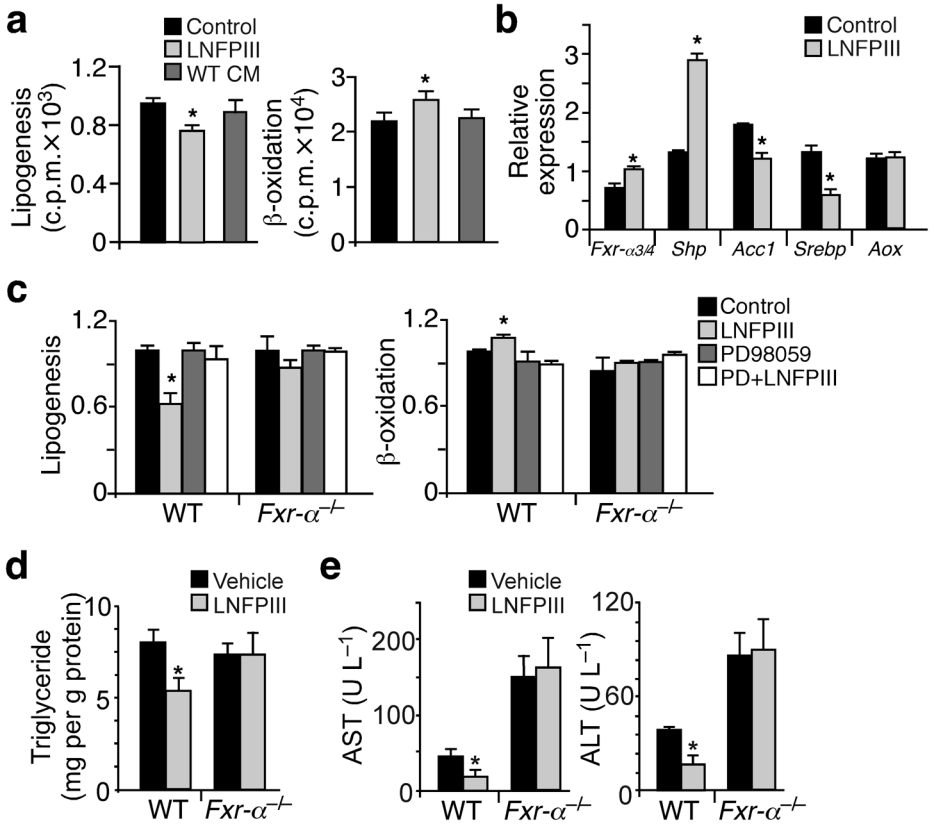

Figure 5.

LNFPIII suppresses lipid synthesis through Fxr-α. (**a**) De novo lipogenesis (left panel) and fatty acid β-oxidation (right panel) assays in primary hepatocytes treated with vehicle, LNFPIII (20 μg ml^{-1}) or CM from LNFPIII primed wt macrophages. (**b**) Gene expression in hepatocytes treated with vehicle or LNFPIII determined by real-time q-PCR. (**c**) Lipogenic (left panel) and β-oxidation (right panel) assays in hepatocytes isolated from wild type (WT) or *Fxr-α*$^{-/-}$ mice ±LNFPIII ±PD98059. (**d** and **e**) Hepatic triglyceride content and serum AST and ALT concentrations in WT and *Fxr-α*$^{-/-}$ mice ±LNFPIII treatment (n = 6). Values are expressed as means ±SEM. For *in vitro* assays, the mean and SEM were determined from 3–4 biological replicates for a representative experiment. Experiments were repeated 3 times. Studies for *Fxr-α*$^{-/-}$ and control mice were conducted in one cohort (n = 6 per treatment per genotype). *P < 0.05 (LNFPIII versus vehicle control).

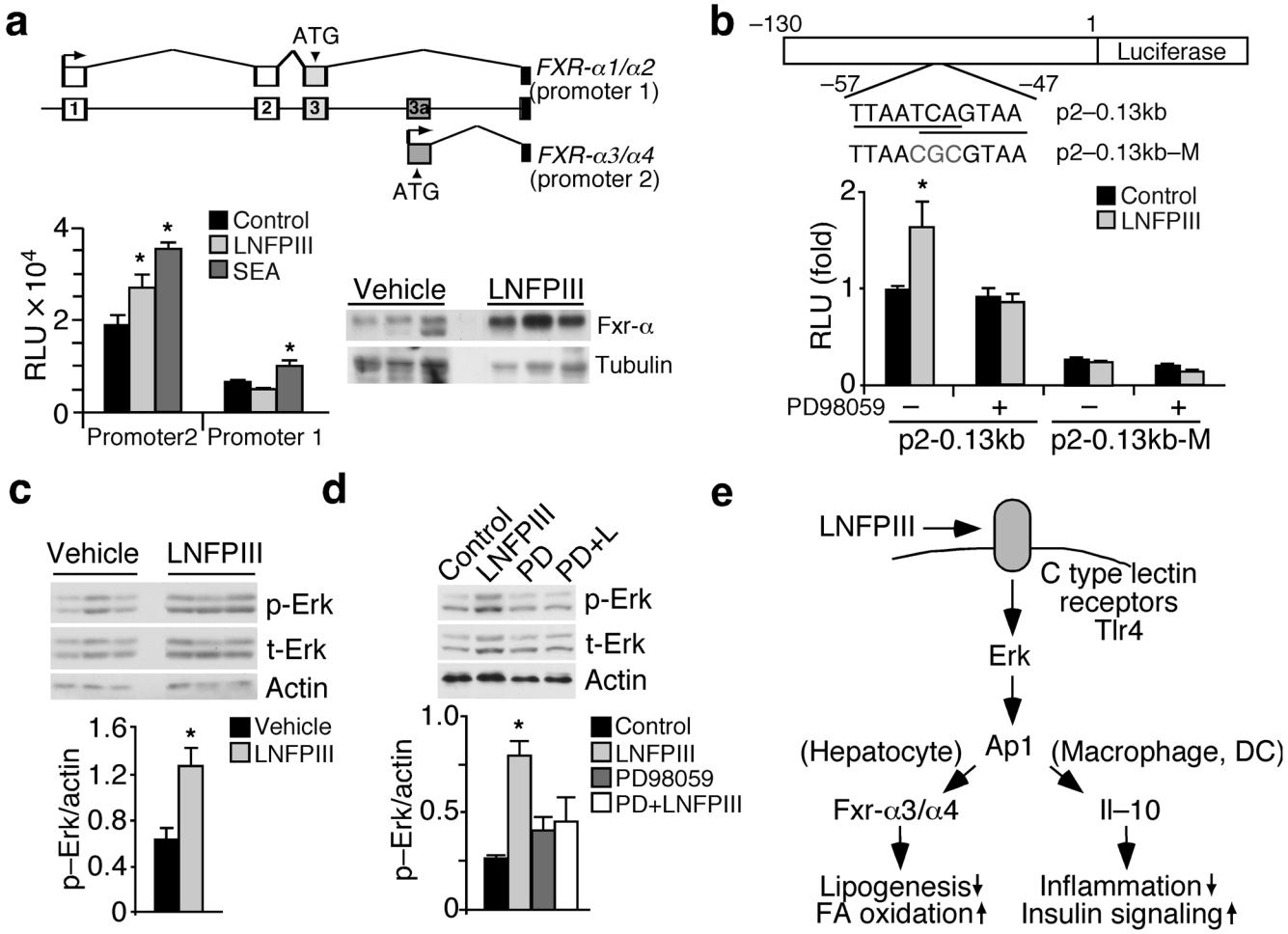

Figure 6.

Induction of Fxr-α activity by LNFPIII is mediated by Erk-Ap1 signaling. (**a**) Top panel: genomic structure showing alternative promoter usage by human *FXR-α1/α2* (promoter 1) and *FXR-α3/α4* (promoter 2). Bottom left: Relative activities (RLU) of luciferase reporters driven by human *FXR-α*promoter 1 (~2 kb) or human *FXR-α*promoter 2 (~0.13 kb) in HepG2 cells ±LNFPIII (20 μg ml^{-1}) or SEA (2 μg ml^{-1}). Bottom right: Western blotting showing Fxr-α protein levels in livers from vehicle or LNFPIII treated mice. (**b**) Top panel: diagram demonstrating *FXR-α* promoter 2 (p2–0.13kb) or mutant (p2–0.13kb–M) reporter constructs. The two overlapping AP1 binding sites and the mutation are shown. Bottom panel: Relative luciferase activities of p2–0.13kb and p2–0.13kb–M ± LNFPIII ± PD98059 (**c**) Erk phosphorylation (p-Erk) in livers of vehicle and LNFPIII treated mice. Bottom panel: Quantification of the Western signal. (**d**) Western blot analyses showing Erk phosphorylation in hepatocytes ± LNFPIII±PD98059 (representative samples from three experiments each with three biological replicates). Bottom panel: Quantification of the Western signal. Values are expressed as means ± SEM. For *in vitro* assays, the mean and SEM were determined from 3–4 biological replicates from one of three repeats. Hepatic p-Erk was determined from one of three metabolic study cohorts ($n = 5$, showing 3 representative samples). *$P < 0.05$ (LNFPIII or SEA versus vehicle control). (**e**) Model for direct and indirect regulation of metabolic pathways by LNFPIII. DC: dendritic cells.